

Bayesian approach to SETI

Claudio Grimaldi^{1,*} and Geoffrey W. Marcy^{2,†}

¹*Laboratory of Physics of Complex Matter, Ecole Polytechnique
Fédérale de Lausanne, Station 3, CP-1015 Lausanne, Switzerland*

²*University of California, Berkeley, CA 94720, USA*

The search for technosignatures from hypothetical galactic civilizations is going through a new phase of intense activity. For the first time, a significant fraction of the vast search space is expected to be sampled in the foreseeable future, potentially bringing informative data about the abundance of detectable extraterrestrial civilizations, or the lack thereof. Starting from the current state of ignorance about the galactic population of non-natural electromagnetic signals, we formulate a Bayesian statistical model to infer the mean number of radio signals crossing Earth, assuming either non-detection or the detection of signals in future surveys of the Galaxy. Under fairly noninformative priors, we find that not detecting signals within about 1 kly from Earth, while suggesting the lack of galactic emitters or at best the scarcity thereof, is nonetheless still consistent with a probability exceeding 10 % that typically over ~ 100 signals could be crossing Earth, with radiated power analogous to that of the Arecibo radar, but coming from farther in the Milky Way. The existence in the Galaxy of potentially detectable Arecibo-like emitters can be reasonably ruled out only if all-sky surveys detect no such signals up to a radius of about 40 kly, an endeavor requiring detector sensitivities thousands times higher than those of current telescopes. Conversely, finding even one Arecibo-like signal within ~ 1000 light years, a possibility within reach of current detectors, implies almost certainly that typically more than ~ 100 signals of comparable radiated power cross the Earth, yet to be discovered.

I. INTRODUCTION

SETI, the search for extraterrestrial intelligence pursued primarily by seeking non-natural electromagnetic (EM) signals in the Galaxy, is notoriously a challenging endeavor with unknown chances of success. Because of the small fraction of the SETI search space explored so far, the non-detections to date of non-natural signals contain only modest informative value about the existence of extraterrestrial technological civilizations in the entire Milky Way. For example, the most recent targeted search for radio transmissions detected no signals in the frequency range between 1.1 and 1.9 GHz from 692 nearby stars, suggesting that fewer than ~ 0.1 % of stars within ~ 160 ly harbor transmitters whose signals cross the Earth and having equivalent isotropic radiated power comparable to or larger than that of terrestrial planetary radars [1]. This fraction drops to about 0.01 % if emitters are assumed to transmit uniformly between ~ 1 and ~ 10 GHz, the frequency range defining the terrestrial microwave window thought to give the best opportunity to detect non-natural EM signals. Extrapolating this result to the entire Galaxy gives a vivid picture of our current state of ignorance. An upper limit of 0.1%-0.01% of stars possessing detectable emitters is indeed consistent with the Earth being illuminated by a total number of radio signals ranging from 0 to 10^6 - 10^7 , even if we consider only sun-like stars with Earth-size planets [2].

This state of extreme uncertainty may however change. The discovery of thousands of extrasolar planets [3] and

the inferred astronomical number of Earth-like planets in the Galaxy[2] have recently stimulated a significant revival of SETI initiatives. The “Breakthrough Listen” project [1, 4], the largest and most comprehensive search ever, and the planned “Cradle of Life” program of the Square Kilometre Array radiotelescope [5, 6], together with impressive progress in detector technology [7, 8], offer unprecedented opportunities for a systematic investigation in the vast domain of the SETI search space.

In view of these rapid developments, exploration of a significant fraction of the Galaxy for a broad range of wavelengths has to be expected in the following years, providing a sufficiently large amount of informative data to infer, at least to some extent, the possible galactic population of non-natural, extraterrestrial signals in the Milky Way.

Here, we report the results of a bayesian analysis formulated by assuming either non-detection or the detection of a signal within a given radio frequency range as a function of the volume of the Galaxy sampled by an hypothetical SETI survey. We construct a statistical model that considers possible populations of extraterrestrial emitters, their spatial and age distributions, and the longevity of the emission processes. By taking into account the luminosity distribution of the emitters and the sensitivities of the detectors, we calculate the posterior probabilities of the average number of signals crossing Earth emitted from the entire Milky Way, given the present very limited level of knowledge. The results show that not detecting signals out to a distance of about 40 kly from Earth places a strong upper limit on the occurrence of detectable EM emissions from the entire Galaxy. This limit can be reached by with future radio telescopes, such as the Phase 2 of the Square Kilometre Array if

* claudio.grimaldi@epfl.ch

† geoff.w.marcy@gmail.com

emitters more powerful than terrestrial planetary radars are assumed. In contrast, the detection of even a single signal from the galactic neighborhood (i.e., within a distance of ~ 1 kly from Earth) hints to a posterior probability of almost 100 % that hundreds of signals from the entire Galaxy typically cross the Earth, with an even larger total number of signals populating the Galaxy.

While our analysis focuses here on radio signals, the formalism can be extended to consider other wavelengths, like the optical and near infrared spectrum searched by some SETI initiatives [9–12]. In the case of short wavelengths, however, absorption and scattering processes have to be considered, as briefly discussed in the concluding section.

II. THE MODEL

In modeling possible galactic populations of non-natural extraterrestrial signals, we start by considering an hypothetical technological, communicating civilization (or emitter) located at some position vector \vec{r} relative to the galactic center. We assume that at some time t in the past the emitter started transmitting, either deliberately or not, an isotropic EM signal, and that the emission process lasted a time interval denoted L . At the present time the region of space occupied by the EM radiation is a spherical shell centered at \vec{r} , with outer radius $R = ct$ and thickness $\Delta = cL$, where c is the speed of light.

A necessary condition for the detection of this signal is that, at the time of observation, the position vector of the Earth, \vec{r}_o , points to a location within the region occupied by the spherical shell, which corresponds to requiring that [13, 14]

$$R - \Delta \leq |\vec{r} - \vec{r}_o| \leq R, \quad (1)$$

where $|\vec{r} - \vec{r}_o|$ is the distance of the emitter from the Earth, Fig. 1. The first inequality of Eq. 1 represents the condition that the last emitted signal of a spherical shell crosses Earth [15]. Since the farthest possible position of a galactic emitter is at the opposite edge of the galactic disk, its maximum conceivable distance from the Earth, $R_M \approx 87$ kly, is simply the sum of the galactic radius (≈ 60 kly*) and the distance of the Earth from the galactic center ($|\vec{r}_o| \approx 27$ kly). Hence, any EM signal emitted before $t_M = R_M/c \approx 87,000$ years from present has already covered a distance larger than R_M , and is therefore absolutely undetectable at Earth. Since

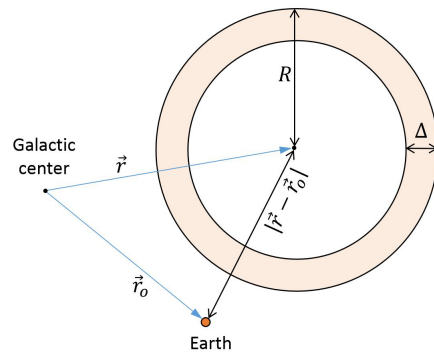


FIG. 1. Two-dimensional schematic representation of a spherical shell signal of outer radius R and thickness Δ . The spherical shell is centered at the emitter location identified by the position vector \vec{r} relative to the galactic center, while the Earth (red circle) is located at \vec{r}_o . In the figure, the Earth lies outside the region covered by the shell, preventing the detection of the signal. The spherical shell signal intercepts the Earth only if the distance emitter-Earth, $|\vec{r} - \vec{r}_o|$, satisfies Eq. 1.

$|\vec{r} - \vec{r}_o| < R_M$, it follows also that the region filled by a spherical shell with outer radius larger than $R_M + \Delta$ cannot contain our planet, regardless of the position of the emitter in the Milky Way. In temporal terms, this means that any emission process lasting L years and that started at a time earlier than $t_M + L$ is unobservable and can be ignored.

A. Probability of shells at Earth

To calculate the probability of signals crossing Earth, we must consider all possible configurations of the spherical shells (their number, position, outer radius and thickness) and identify those that satisfy Eq. 1. To this end, we first discard any unobservable signal by assigning to a randomly chosen star a probability q of harboring an emitter that has been actively transmitting some time within t_M years from present. The mean number of such emitters is thus qN_s , where N_s is the number of stars in the Galaxy. We make the additional assumption that the starting time and the duration of the emissions (or, equivalently, the outer radius and the thickness of the spherical shells) are independent and identically distributed random variables, t and L , with probability density functions (PDFs) given by $\rho_t(t)$ and $\rho_L(L)$, respectively, and that the signal frequencies are distributed uniformly within a given range. The resulting probability p that the Earth intersects a signal under the condition that it is no older than t_M (or, equivalently, that the emission process started within a time $t_M + L$ before

* Here we adopt the presumption that stars that can potentially harbor emitters are rich in heavy elements, so to favor the formation of rocky planets. 60 kly is approximately the radius of the galactic thin disk (see Sec. IV) which is a metal-rich component of the Milky Way. The contribution of farther stars [16, 17] and/or other galactic components [18] can nonetheless be incorporated by the present formalism

present) is therefore [13]

$$p = q \frac{\int dL \rho_L(L) \int_0^{t_M+L} dt \rho_t(t) \int d\vec{r} \rho_s(\vec{r}) f_{R,\Delta}(\vec{r} - \vec{r}_o)}{N_s \int dL \rho_L(L) \int_0^{t_M+L} dt \rho_t(t)}, \quad (2)$$

where $f_{R,\Delta}(\vec{r} - \vec{r}_o) = 1$ if Eq. 1 is satisfied and $f_{R,\Delta}(\vec{r} - \vec{r}_o) = 0$ otherwise, and $\rho_s(\vec{r})$ is the star number density function. For the moment, we do not need to specify its detailed form and require only that $\int d\vec{r} \rho_s(\vec{r}) = N_s$ and that $\rho_s(\vec{r})$ has approximately a disk-like shape with a radius of about 60 kly.

Assuming the steady-state condition that over a time span of order t_M from present the PDF of the starting time of emission, $\rho_t(t)$, is essentially constant [13], the integrals over t in Eq. 2 can be solved exactly and p reduces simply to (SI Appendix, Section I):

$$p = q\lambda \equiv q \frac{\bar{L}}{\bar{L} + t_M}, \quad (3)$$

where the second equality defines the scaled longevity of the signal, λ , and $\bar{L} = \int dL \rho_L(L) L$ denotes the average duration of the signal. Finally, from Eq. 3 we obtain the mean number of signals crossing Earth,

$$\bar{k} = q\lambda N_s, \quad (4)$$

which has to be understood as a statistical average over all configurations of the emitted signals.[†]

\bar{k} is the quantity of main interest here for two reasons. First, Eq. 4 expresses the two unknown quantities λ and q in terms of a single parameter, \bar{k} , which, as shown in the following, can be in principle inferred by observations. As emphasized in Fig. 2, knowledge of \bar{k} , or at least plausible upper or lower bounds, would also enable via Eq. 4 an estimate of the mean number qN_s of shell signals occupying the Galaxy as a function of the mean signal longevity. For example, $\bar{k} \sim 1$ implies that qN_s can be as large as ~ 1000 if $\bar{L} \sim 100$ years is assumed, although in this case the vast majority of the signals do not cross the Earth.

Second, under the steady-state hypothesis, \bar{k} coincides with the average number of emitters that are *currently* radiating isotropic signals (SI Appendix, Section I). In particular, \bar{k} can be shown to coincide with \bar{L}/τ [14], where τ^{-1} , the average birthrate of emitters, effectively incorporates the different probability factors appearing in the Drake equation [19, 20]. An informed estimate of \bar{k} would bring therefore a valuable knowledge about the potential abundance of presently active emitters in the Galaxy.

[†] For example, values of \bar{k} smaller or much smaller than ~ 1 imply that configurations with signals crossing Earth are rare or very rare.

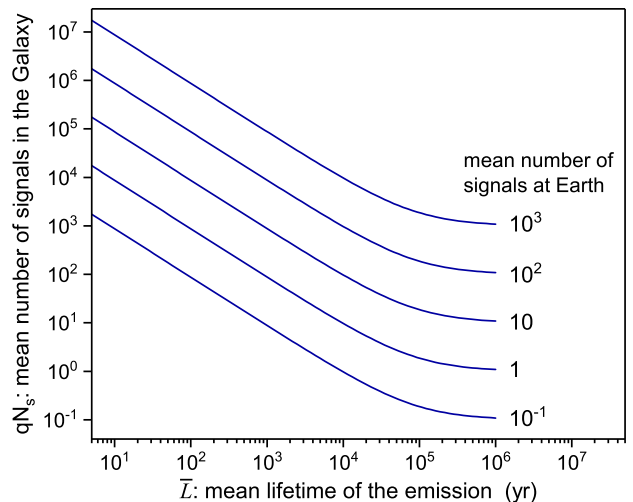


FIG. 2. Relation between the average number of spherical shell signals present in the Galaxy, qN_s , and the mean signal longevity \bar{L} . The value of qN_s for given \bar{L} is determined by \bar{k} , the average number of signals crossing Earth, through $qN_s = \bar{k}(\bar{L} + t_M)/\bar{L}$, where t_M is the age of the oldest signal which could possibly cross our planet.

B. Signal detectability

In deriving Eq. 4, we have considered possible galactic populations of isotropic signals without referring to their actual detectability by means of terrestrial, dedicated telescopes used in observational surveys. Even in the hypothesis that our planet lies in a region covered by the signals, their detection actually depends on a number of factors such as the distance of the emitters, their radiated power, the wavelength of the signals, the minimum sensitivity of the detectors, and the search strategy.

To illustrate how these factors influence the detectability of extraterrestrial signals, we consider here the case in which a SETI search is designed to scan the entire sky for radio signals within a given range of frequencies. Contrary to targeted searches, in which a discrete set of target stars is selected, an all-sky survey covers in principle all directions of the sky. In this case the search space is a sphere centered at Earth of radius specified by the radiated power of the emitter and by the detector sensitivity. To see this, we assume that an emitter at \vec{r} that transmits within a given range of radio frequencies has intrinsic luminosity L (not to be confused with L , the signal longevity) and that in the same frequency range the detector (i.e., the radiotelescope) has a minimum detectable flux denoted S_{\min} . Since the flux received by the detector is inversely proportional to the square of the distance from the source, the emitter is instrumentally detectable as long as its distance from the Earth is such that

$$L \geq 4\pi |\vec{r} - \vec{r}_0|^2 S_{\min}. \quad (5)$$

The detection of an isotropic signal requires therefore that the conditions 1 and 5 must be simultaneously fulfilled. The resulting detection probability amounts to multiply $f_{R,\Delta}(\vec{r}-\vec{r}_o)$ in Eq. 2 by $\theta(R_L - |\vec{r}-\vec{r}_o|)$, where $\theta(x) = 1$ if $x \geq 0$ and $\theta(x) = 0$ if $x < 0$, and

$$R_L = \sqrt{\frac{L}{4\pi S_{\min}}} \quad (6)$$

is the distance beyond which an emitter with intrinsic luminosity L is instrumentally undetectable. After the integrals over L and t in Eq. 2 are performed under the steady-state condition, the detection probability of a single signal reduces to:

$$p' = \frac{q}{N_s} \lambda \int d\vec{r} \rho_s(\vec{r}) \theta(R_L - |\vec{r}-\vec{r}_o|), \quad (7)$$

from which we recover Eq. 3 by choosing values of L/S_{\min} large enough to make R_L bigger than R_M , the maximum distance of an emitter from Earth.

Although S_{\min} is a known parameter that depends on the instrumental characteristics of the detector, the intrinsic luminosity of the emitter, L , is an unknown quantity, which we treat probabilistically by introducing a PDF of the luminosity (commonly denoted luminosity function), $g(L)$, independent of the duration of the emission process. We replace therefore the detection probability given in Eq. 7 by $p' = q\lambda\pi_o(R_{L^*})$, where

$$\pi_o(R_{L^*}) = \frac{1}{N_s} \int_0^{L^*} dL g(L) \int d\vec{r} \rho_s(\vec{r}) \theta(R_L - |\vec{r}-\vec{r}_o|) \quad (8)$$

is the luminosity detection probability. Although not strictly necessary, we have assumed in Eq. 8 that $g(L)$ vanishes for luminosities larger than a maximum value, L^* . In this way, Eq. 8 implies that an emitter that is outside a sphere centered on Earth and of radius

$$R_{L^*} = \sqrt{\frac{L^*}{4\pi S_{\min}}} \quad (9)$$

is instrumentally undetectable, even if the emitted shell intersects the Earth. Note that since we take $\rho_s(\mathbf{r})$ to be approximately disk-like, the luminosity detection probability resulting from a SETI survey of the sky around the galactic plane, instead of an all-sky survey, is not expected to differ significantly from Eq. 8.

Given $p' = q\lambda\pi_o$, where π_o is a short-hand notation for $\pi_o(R_{L^*})$, and assuming that the emitters have the same luminosity function, the probability that a telescope involved in the all-sky survey detects exactly $k = 0, 1, 2 \dots, N_s$ spherical shell signals reduces to a binomial distribution:

$$p(k|\pi_o) = \binom{N_s}{k} p'^k (1-p')^{N_s-k}. \quad (10)$$

The average number of signals that can be detected by the survey is therefore $\sum_{k=0}^{N_s} k p(k|\pi_o) = p' N_s = \pi_o \bar{k}$,

where \bar{k} is the mean number of signals at Earth given in Eq. 4. Finally, noting that the value of N_s inferred from the analysis of the data from the Kepler space telescope is in the order of tens of billions [2], Eq. 10 can be conveniently approximated by a Poisson distribution as long as k and $\pi_o \bar{k}$ are much smaller than $N_s \approx 10^{10}$. We write therefore:

$$p(k|\pi_o) = \frac{(\pi_o \bar{k})^k}{k!} e^{-\pi_o \bar{k}}, \quad (11)$$

which completes the definition of our model. In the following Bayesian analysis, we will use Eq. 11 to derive the likelihood functions corresponding to possible outcomes of a SETI search.

III. BAYESIAN ANALYSIS

Bayes' theorem provides a recipe for updating an initial hypothesis about the probability of occurrence of an event in response to new evidence [21]. Here, we take the initial hypothesis that the Earth intersects with a prior probability distribution $p(\bar{k})$ an average number $\bar{k} \geq 0$ of signals emitted from communicating civilizations in the Galaxy, regardless of whether we detect them or not.

Let us suppose that new evidence on the number of detected signals (evidence \mathcal{E}) emerges from the acquisition of new data in a SETI survey. Bayes' theorem states that the posterior probability that there are in average \bar{k} signals intercepting our planet taking into account the evidence \mathcal{E} is:

$$p(\bar{k}|\mathcal{E}) = \frac{p(\mathcal{E}|\bar{k})p(\bar{k})}{p(\mathcal{E})}, \quad (12)$$

where $p(\mathcal{E}) = \int d\bar{k} p(\mathcal{E}|\bar{k})p(\bar{k})$, the marginal likelihood of \mathcal{E} , is a normalization constant and $p(\mathcal{E}|\bar{k})$ is the likelihood function defined as the conditional probability that the event \mathcal{E} occurs given the initial hypothesis about \bar{k} .

A. Likelihood terms

For the sake of simplicity, we shall not discuss here the occurrence of false positive or false negative results from an all-sky SETI survey, and we consider the only two possible outcomes, that is, a negative result for signal detection or a positive evidence for the existence of communicating civilizations represented by the detection of one signal.

In the first case we assume that an observational campaign as the one described in Sec. II has detected no signals within the entire sky (and within a depth set by R_{L^*}). Let \mathcal{E}_0 denote this evidence. The corresponding likelihood function, $p(\mathcal{E}_0|\bar{k})$, is obtained by setting $k = 0$ in Eq. 11,

$$p(\mathcal{E}_0|\bar{k}) = e^{-\pi_o \bar{k}}. \quad (13)$$

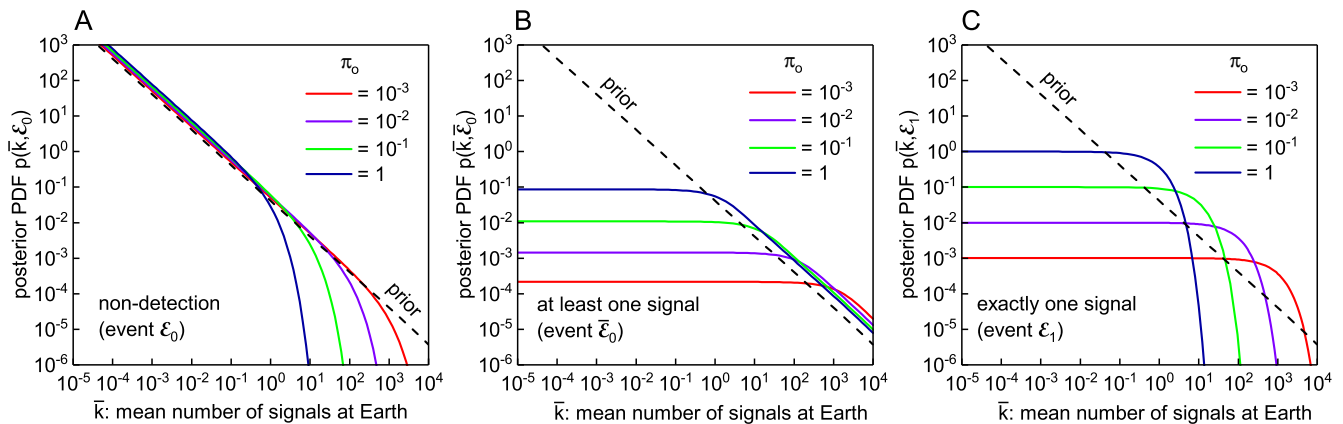


FIG. 3. Probability distribution functions (PDFs) of the mean number of shell signals crossing Earth, \bar{k} , for different values of the luminosity detection probability π_o . The dashed and solid lines represent respectively the prior and posterior PDFs resulting from A: no signal detection (event \mathcal{E}_0), B: at least one detectable signal (event $\bar{\mathcal{E}}_0$), C: exactly one detectable signal (event \mathcal{E}_1). In A and B the posterior PDFs are smaller than the prior when, respectively, $\bar{k} > 1/\pi_o$ and $\bar{k} < 1/\pi_o$, whereas in C the weight of the posterior PDF is concentrated mostly around $\bar{k} \sim 1/\pi_o$.

Quite intuitively, Eq. 13 shows that for $\pi_o \neq 0$ the probability of \mathcal{E}_0 occurring decays exponentially with \bar{k} , implying that values of \bar{k} much larger than $1/\pi_o$ can be ruled out by the non-detection of signals.

In considering the case that an all-sky SETI survey detects a non-natural, extraterrestrial signal, we need to distinguish between two possibilities depending on whether the gathered evidence can exclude or not the existence of detectable signals from other emitters within R_{L^*} (besides the one already detected). This distinction has to be made because the detection may occur before the sky has been entirely swept out, not excluding therefore the possibility that there may be other detectable signals from emitters within R_{L^*} . In this case the evidence, denoted $\bar{\mathcal{E}}_0$, is that there is *at least one* detectable signal emitted within a distance R_{L^*} . The associated likelihood is $p(\bar{\mathcal{E}}_0|\bar{k}) = 1 - p(\mathcal{E}_0|\bar{k})$ because $\bar{\mathcal{E}}_0$ is the negation of \mathcal{E}_0 , the event of non-detection considered above. Hence

$$p(\bar{\mathcal{E}}_0|\bar{k}) = 1 - e^{-\pi_o \bar{k}}. \quad (14)$$

The second possibility is that the evidence, denoted \mathcal{E}_1 , amounts to detect *exactly one* emitter in the entire sky within a depth R_{L^*} , as it would be the case if no other signals have been detected upon the completion of the survey. The likelihood term in this case is therefore given by Eq. 11 with $k = 1$:

$$p(\mathcal{E}_1|\bar{k}) = \pi_o \bar{k} e^{-\pi_o \bar{k}}. \quad (15)$$

Since the likelihoods 14 and 15 are significant when, respectively, $\pi_o \bar{k} \gtrsim 1$ and $\pi_o \bar{k} \sim 1$, large values of \bar{k} have to be expected when π_o is small. In other terms, the smaller the fraction of the Galaxy in which a SETI survey is successful, the larger is the likely number of broadcasting emitters in the Milky Way.

B. Prior distribution

To obtain the posterior probability $p(\bar{k}|\mathcal{E})$, $\mathcal{E} = \mathcal{E}_0, \mathcal{E}_1$, and $\bar{\mathcal{E}}_0$, we need to specify $p(\bar{k})$, the prior probability distribution of \bar{k} . Presently, we lack generally accepted arguments to estimating either the fraction q of stars in the Galaxy that may harbor communicating civilizations, or the mean signal longevity \bar{L} . Possible values of \bar{k} may therefore range from $\bar{k} = 0$, as argued by proponents of the rare Earth hypothesis [22], to a significant fraction of N_s , in the most optimistic scenarios.

A natural choice of $p(\bar{k})$, befitting our ignorance about even the scale of \bar{k} , would be taking a prior PDF that is uniform in $\log(\bar{k})$, which corresponds to $p(\bar{k}) \propto \bar{k}^{-1}$, to give equal weight to all orders of magnitude [21, 23].[‡] Although the log-uniform prior appropriately expresses our state of ignorance, it fails to take into account that, after all, various past SETI surveys have been conducted since several decades [24], with null results. Likewise, there have been no serendipitous detection of non-natural extraterrestrial signals since the invention of radio telescopes.

To allow the prior PDF to reflect the so far lack of detection, we introduce a prior luminosity detection probability defined as $\pi_o^{\text{prior}} = \pi_o(R_{L^*}^{\text{prior}})$, where $R_{L^*}^{\text{prior}}$, the prior observational radius, is representative of the distance accessible by past SETI surveys for given values of L^* and frequency range. The likelihood of non-detection, Eq. 13, immediately suggests that a natural way to inform the prior about past SETI negative results is to update $p(\bar{k})$ using Bayes' theorem, leading

[‡] At first sight, a prior PDF uniform in \bar{k} appears to reflect our state of ignorance. It is however a highly informative prior because it strongly favors large values of \bar{k} [23].

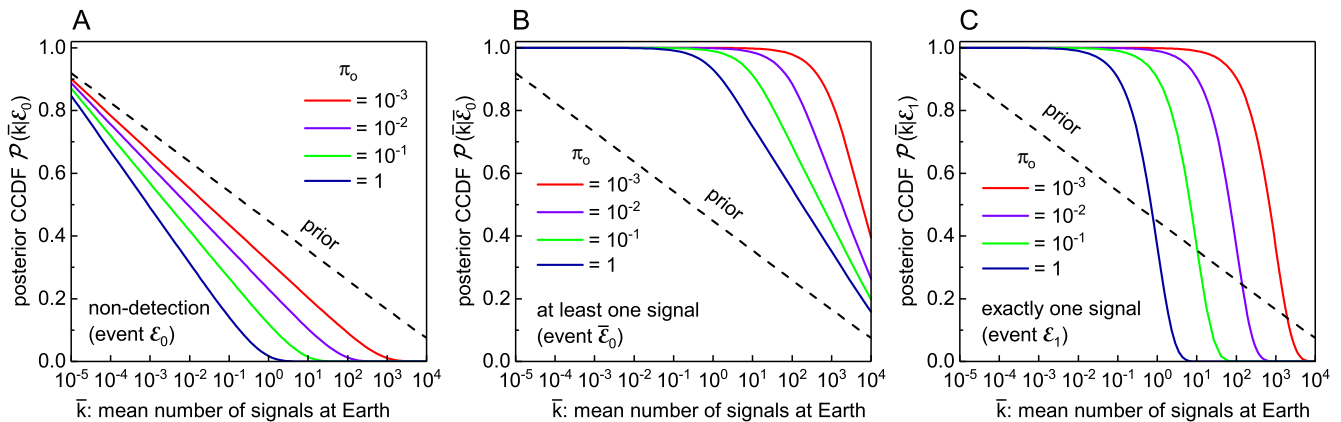


FIG. 4. Complementary cumulative distribution functions (CCDFs) of \bar{k} for different values of the luminosity detection probability π_o . Each curve gives the probability that the mean number of signals intersecting Earth’s orbit is larger than \bar{k} . The dashed and solid lines represent respectively the prior and posterior CCDFs resulting from A: no signal detection (event \mathcal{E}_0), B: at least one detectable signal (event $\bar{\mathcal{E}}_0$), C: exactly one detectable signal (event \mathcal{E}_1). In A the posterior CCDF becomes progressively smaller than the prior as π_o increases, and it vanishes exponentially for $\bar{k} > 1/\pi_o$. In B and C the posterior CCDFs deviate more from the prior when π_o is smaller. For $\pi_o = 10^{-3}$ the posterior probability that there are more than 100 signals intercepting the Earth is larger than 95 %.

to $p(\bar{k}) \propto \bar{k}^{-1} \exp(-\pi_o^{\text{prior}} \bar{k})$. In so doing, we are simply adopting as prior the posterior PDF resulting from the non-detection of signals of past SETI initiatives. Finally, in order to make the prior distribution proper (i.e., normalizable) we introduce a lower cut-off in \bar{k} so that $p(\bar{k}) = 0$ when $\bar{k} < \bar{k}_{\text{min}}$. The normalized prior distribution becomes therefore

$$p(\bar{k}) = \frac{\bar{k}^{-1} e^{-\pi_o^{\text{prior}} \bar{k}}}{E_1(\pi_o^{\text{prior}} \bar{k}_{\text{min}})} \theta(\bar{k} - \bar{k}_{\text{min}}), \quad (16)$$

where $E_1(x) = \int_x^\infty dt e^{-t}/t$ is the exponential integral. The value of \bar{k}_{min} can be chosen so as to satisfy some appropriate criterion. Here we adopt the requirement that \bar{k}_{min} gives the least informative prior probability that at least one signal from the entire Galaxy intercepts Earth’s orbit, leading to $\bar{k}_{\text{min}} \simeq 0.14 \pi_o^{\text{prior}}$ (SI Appendix, Section II).

C. Posterior probabilities

The normalized product of the prior probability distribution 16 with each of the three likelihood functions 13, 14, and 15 gives the respective PDFs resulting from the events \mathcal{E}_0 (non-detection), $\bar{\mathcal{E}}_0$ (at least one detection), and \mathcal{E}_1 (exactly one detection). To keep the analysis as general as possible, for the moment we treat the luminosity detection probability, π_o , as an independent variable ranging between 0 and 1. We shall restore its full dependence upon the observational radius R_{L^*} in the section dedicated to the discussion of present and future SETI surveys. For illustrative purposes, we also take π_o^{prior} constant and equal to 10^{-5} , a value not far from our

subsequent estimates of the prior luminosity detection probability.

Figure 3 compares the PDFs of \bar{k} (solid lines), calculated for different values of π_o , with the prior distribution (dashed lines). There are three relevant features worth to be stressed. First, all three posteriors are manifestly driven by their respective data (\mathcal{E}_0 , $\bar{\mathcal{E}}_0$, and \mathcal{E}_1) and not the prior, confirming that the latter is fairly non-informative. Second, the posterior PDF resulting from the event of non-detection, Fig. 3A, converges smoothly to the prior PDF as $\pi_o \rightarrow 0$, and deviates most from it when $\bar{k} > 1/\pi_o$, as anticipated by the likelihood term 13. A substantial effect of the datum (that is, the event of non-detection) is expected therefore only for π_o significantly larger than π_o^{prior} . Finally, the third significant result is that the posterior PDFs resulting from the detection of a signal, Fig. 3B and 3C, do not converge to the prior for $\pi_o \rightarrow 0$. In this limit, the corresponding likelihood terms 14 and 15 are proportional to \bar{k} , which cancels the factor \bar{k}^{-1} of the prior. Consequently, for $\bar{k} \lesssim 1/\pi_o$ the posterior PDFs $p(\bar{k}|\bar{\mathcal{E}}_0)$ and $p(\bar{k}|\mathcal{E}_1)$ are approximately constant, and get progressively small as π_o diminishes. This has the net effect of shifting the weight of $p(\bar{k}|\bar{\mathcal{E}}_0)$, Fig. 3C, to $\bar{k} > 1/\pi_o$ and, due to the cutoff at $\bar{k} > 1/\pi_o$ in the likelihood term associated to \mathcal{E}_1 , of concentrating the weight of $p(\bar{k}|\mathcal{E}_1)$ in the region around $\bar{k} \sim 1/\pi_o$, Fig. 3C. Therefore, in case of detection, the smaller the value of π_o (or, equivalently, the smaller the observational radius R_{L^*}) the larger is the probability that the Earth intersects many shell signals other than the one already detected.

By integrating the posterior PDFs from \bar{k} to ∞ , we calculate the complementary cumulative distribution functions (CCDFs), which give the updated probabilities that

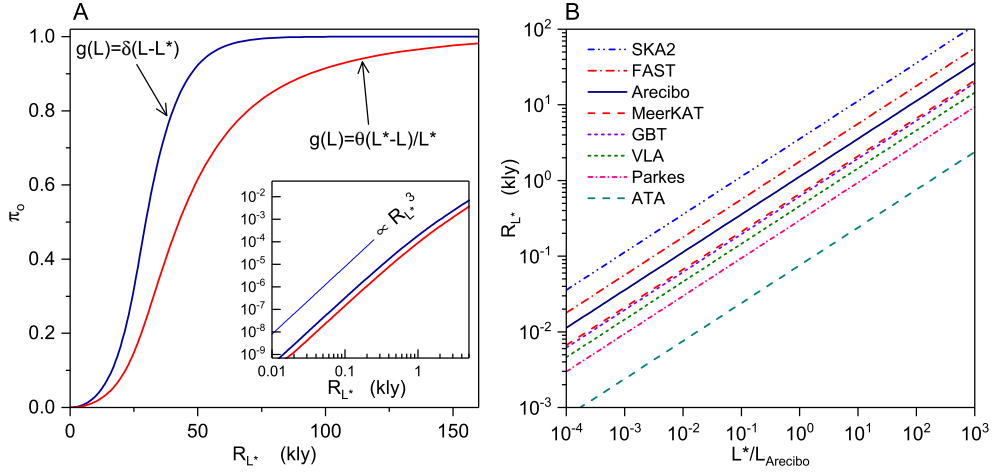


FIG. 5. A: Probability π_o that an emitter is within an observable sphere of radius R_{L^*} for the cases in which the emitter luminosity function is either a single Dirac-delta peak centered at L^* or a uniform distribution extending up to L^* . The inset shows that within the galactic neighborhood ($R_{L^*} \lesssim 1$ kly) π_o scales as $R_{L^*}^3$. B: Radius of the observable sphere for several telescopes as a function of the intrinsic luminosity of an emitter in units of $L_{\text{Arecibo}} = 2 \times 10^{13}$ W, the equivalent isotropic radiated power of the Arecibo radar. The values of the minimum detectable flux (S_{min}) are reported in Table I for each telescope. Note that from Eq. 9 R_{L^*} scales as $\sqrt{L^*}$.

the mean number of shells intersecting Earth, transmitted from the entire Galaxy, is larger than \bar{k} . For each event \mathcal{E}_0 , $\bar{\mathcal{E}}_0$, and \mathcal{E}_1 , the CCDFs are given respectively by:

$$\mathcal{P}(\bar{k}|\mathcal{E}_0) = \int_{\bar{k}}^{\infty} d\bar{k}' p(\bar{k}'|\mathcal{E}_0) = \frac{E_1[(\pi_o + \pi_o^{\text{prior}})\bar{k}]}{E_1[(\pi_o + \pi_o^{\text{prior}})\bar{k}_{\text{min}}]}, \quad (17)$$

$$\begin{aligned} \mathcal{P}(\bar{k}|\bar{\mathcal{E}}_0) &= \int_{\bar{k}}^{\infty} d\bar{k}' p(\bar{k}'|\bar{\mathcal{E}}_0) \\ &= \frac{E_1(\pi_o^{\text{prior}}\bar{k}) - E_1[(\pi_o + \pi_o^{\text{prior}})\bar{k}]}{E_1(\pi_o^{\text{prior}}\bar{k}_{\text{min}}) - E_1[(\pi_o + \pi_o^{\text{prior}})\bar{k}_{\text{min}}]}, \quad (18) \end{aligned}$$

$$\mathcal{P}(\bar{k}|\mathcal{E}_1) = \int_{\bar{k}}^{\infty} d\bar{k}' p(\bar{k}'|\mathcal{E}_1) = e^{-(\pi_o + \pi_o^{\text{prior}})(\bar{k} - \bar{k}_{\text{min}})}. \quad (19)$$

Figure 4 shows Eqs. 17-19 (solid lines) for the same values of π_o of Fig. 3. The prior CCDF (dashed lines) is obtained by setting $\pi_o = 0$ in Eq. 17. As anticipated by the analysis of the PDFs, the posterior CCDFs resulting from the non-detection or a detection of a signal differ significantly from each other. While the response to \mathcal{E}_0 , Fig. 4A, becomes progressively smaller than the prior as π_o increases, and getting negligibly small for $\bar{k} > 1/\pi_o$, the posterior CCDFs resulting from the detection of a signal (either event $\bar{\mathcal{E}}_0$ or \mathcal{E}_1) depart abruptly from the prior CCDF as soon as $\pi_o \neq 0$, as shown in Figs. 4B and 4C. In particular, for a relatively small value of π_o (say for example $\sim 10^{-3}$) the detection of at least one signal (event $\bar{\mathcal{E}}_0$) implies that the posterior probability that the Earth intersects typically more than $\bar{k} \sim 1/\pi_o \sim 10^3$ signals exceeds $\sim 80\%$. This probability drops to about

35% if exactly one signal is detected in the entire sky for the same value of π_o (event \mathcal{E}_1 , Fig. 3c). Since $\mathcal{P}(\bar{k}|\bar{\mathcal{E}}_0)$ and $\mathcal{P}(\bar{k}|\mathcal{E}_1)$ represent respectively an upper and lower limit for the posterior probability in the case of detection, the probability that there are in average more than 10^3 galactic signals crossing the Earth is therefore comprised between $\sim 80\%$ and $\sim 35\%$ in this example.

IV. BAYESIAN ANALYSIS APPLIED TO EXISTING AND UPCOMING SETI DETECTORS

We now apply our Bayesian formalism by considering existing and planned radiotelescopes to infer the posterior probabilities following the potential occurrence of events \mathcal{E}_0 , $\bar{\mathcal{E}}_0$, and \mathcal{E}_1 in a SETI survey. The quantity governing the response to these events is $\pi_o(R_{L^*})$, the probability that an emitter is within a distance R_{L^*} from the Earth. According to Eq. 8, this quantity depends on the number distribution of stars, $\rho_s(\vec{r})$, and the luminosity function of the emitters, $g(L)$. The latter identifies also the observational radius, R_{L^*} , once a specific telescope sensitivity is assigned.

A. Number density of stars

We take the number density function $\rho_s(\vec{r})$ to have a cylindrical symmetry of the form:

$$\rho_s(\vec{r}) = \rho_0 e^{-r/r_s} e^{-|z|/z_s} \quad (20)$$

where r is the radial distance from the galactic center, z is the height from the galactic plane, and ρ_0 is a normal-

TABLE I. System equivalent flux density, S_{sys} , and corresponding sensitivity, S_{min} , for the Allen Telescope Array (ATA) [1, 25], the Parkes telescope [1], the Jansky Very Large Array telescope (VLA) [1, 26], the Green Bank Telescope (GBT) [1], the Meer Karoo Array Telescope (MeerKAT) [27], the Arecibo telescope [28], the Five hundred meter Aperture Spherical Telescope (FAST) [29], and the Phase 2 of the Square Kilometre Array (SKA2) [30]. The values of S_{min} are calculated from Eq. 21 assuming $m = 15$, $\Delta\nu = 0.5$ Hz, and $t = 10$ min.

telescope	S_{sys} (Jy)	S_{min} (10^{-26} W/m ²)
ATA	664 ^a	287
Parkes	43	18.6
VLA	18	7.8
GBT	10	4.3
MeerKAT	8.6	3.7
Arecibo	3	1.3
FAST	1.2	0.5
SKA	0.3 ^b	0.13

^a SEFD for 27 antennas

^b Estimate of the goal value the SEFD (frequency range ~ 1 -2 GHz) targeted upon completion of the phase 2 of the SKA telescope [30]. See

<https://astronomers.skatelescope.org/documents> for further documentation on phase 1, phase 2, and precursors of SKA.

ization factor ensuring that $\int d\vec{r} \rho_s(\vec{r}) = N_s$. We assume that the emitters are potentially located in the thin disk of the Milky Way, whose star distribution follows approximately Eq. 20 with $r_s = 8.15$ kly and $z_s = 0.52$ kly [31]. The resulting $\rho_s(\vec{r})/N_s$ gives a probability over 99 % of finding a star at a distance of 60 kly from the galactic center.[§]

B. Luminosity function

Since we ignore what a plausible PDF of L looks like, and whether it even exists, modeling the luminosity function $g(L)$ unavoidably requires making some assumptions. Previously, a power-law distribution of the form $g(L) \propto L^{-\alpha}$ has been proposed as a vehicle to assess, through the choice of the exponent α , the interplay between the proximity of a detectable emitter and its spectral density [33, 34]. Here, we limit our analysis to the effect on the detection probability of the spread of the luminosity distribution by considering some limiting forms of $g(L)$. To this end, we take $g(L)$ to be given either by a single Dirac-delta peak centered at some characteristic

[§] We have considered also the possibility that the distribution of stars that can potentially harbor life has an annular shape, as in the galactic habitable zone proposed in Ref. [32] (SI Appendix, Section 3).

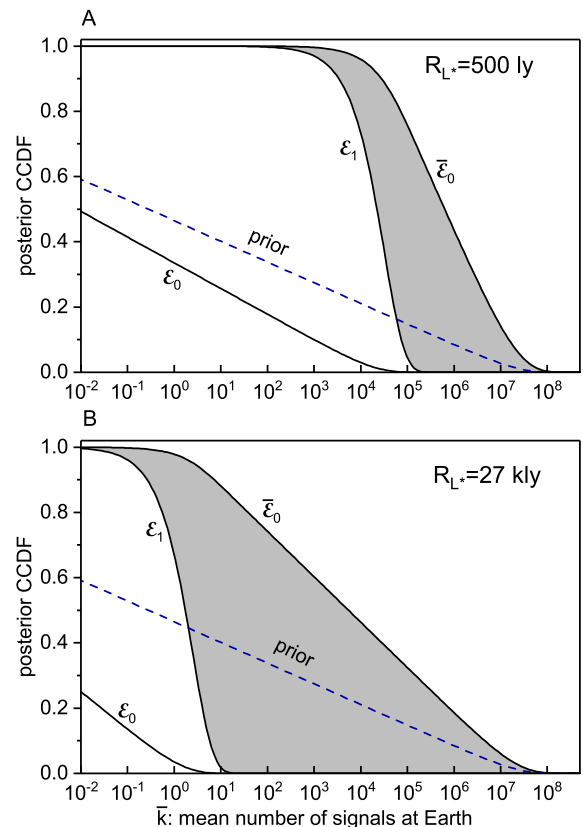


FIG. 6. Posterior CCDFs giving the probabilities that the mean number of signals crossing Earth is larger than \bar{k} . The solid curves refer to the CCDFs resulting from the events of non-detection (\mathcal{E}_0), at least one detectable signal ($\bar{\mathcal{E}}_0$), and exactly one detectable signal (\mathcal{E}_1) within 500 ly from Earth (A), corresponding to an observational radius containing about one million nearby stars targeted by the “Break-through Listen” project, or within 27 kly from Earth (B), that is the distance to the galactic center. The dashed line denotes the prior CCDF calculated as described in the text. The results are computed by adopting a delta-Dirac luminosity function for the emitters centered at $L^* = L_{\text{Arecibo}}$, where $L_{\text{Arecibo}} = 2 \times 10^{13}$ W is the equivalent isotropic radiated power (EIRP) of the Arecibo radar.

luminosity L^* , $g(L) = \delta(L - L^*)$, or by a uniform distribution ranging from $L = 0$ up to L^* : $g(L) = \theta(L^* - L)/L^*$. In either case, the dependence of π_o on the width of the luminosity function can be conveniently expressed in terms of the maximum detectable distance, R_{L^*} , Eq. 9, as illustrated in Fig. 5A. While at distances of about $R_M \sim 90$ kly or larger, π_o saturates to one due to the finite size of the Galaxy, in the galactic neighborhood ($R_{L^*} \lesssim 1$ kly) the function π_o is smaller than about 10^{-3} and it scales as $R_{L^*}^3$, inset of Fig. 5A.

C. Observational radius

To determine the observational radius R_{L^*} , Eq. 9, of an all-sky SETI survey, we must specify the characteristic luminosity of the emitters, L^* , and the minimum detectable flux, S_{\min} . The latter quantity is determined by the characteristics of the telescope used in the SETI search and the intrinsic bandwidth of the transmitted signal. Here, we consider the case of a signal bandwidth narrower than the spectral resolution of the telescope, which reduces S_{\min} to [1, 26]:

$$S_{\min} = m S_{\text{sys}} \sqrt{\frac{\Delta\nu}{t}}, \quad (21)$$

where m is the desired signal-to-noise ratio, t is the integration time in seconds, $\Delta\nu$ is the receiver channel bandwidth (expressed in Hz), and S_{sys} is the system equivalent flux density (SEFD), which depends on the system temperature of the receiver and on the effective collecting area of the telescope. Table I lists the values of S_{sys} in Jy (1 Jy = 10^{-26} Wm⁻²Hz⁻¹) of a few existing and planned facilities [1, 6, 25–29] and the corresponding S_{\min} in Wm⁻² calculated for $m = 15$, $\Delta\nu = 0.5$ Hz, and $t = 600$ s. In Table I, the SEFD values of ATA, Parkes, VLA, GBT, and Arecibo refer to past targeted searches for non-natural radio signals of frequencies comprised between ~ 1 and ~ 2 GHz, while those attributed to MeerKAT, FAST and SKA2 are only indicative, as these telescopes are either not yet fully operational (MeerKAT and FAST) or still in the study phase (SKA2).

Figure 5B shows the values of R_{L^*} that the telescopes enlisted in Table I, or other facilities of comparable sensitivity, could access if they were employed in an all-sky search for signals within ~ 1 -2 GHz. From Figs. 5A and 5B we see that for $L^*/L_{\text{Arecibo}} \lesssim 0.1$, where $L_{\text{Arecibo}} = 2 \times 10^{13}$ W is the equivalent isotropic radiated power (EIRP) emitted by the Arecibo radar,[¶] even the most sensitive receiver (the planned phase 2 of the SKA telescope) can probe distances only up to about 1 kly, where the probability π_o is small, while $L^*/L_{\text{Arecibo}} \gtrsim 100$ has to be assumed to make π_o significant.

D. Prior parameters

To assign the probability π_o^{prior} that has to be plugged into the prior PDF 16, we have to estimate the observational radii within which no emitters have been detected so far, assuming given EIRP values of the emitters. The

[¶] Although this value of the EIRP refers to the Arecibo radar transmitting at a frequency of 2.38 GHz, which is outside the observational frequency coverage considered here (about 1-2 GHz), we nonetheless adopt $L_{\text{Arecibo}} = 2 \times 10^{13}$ W as a useful term of comparison, as the Arecibo radar is the most powerful radio transmitter on Earth.

best strategy is probably to adopt a value of S_{\min} , denoted S_{\min}^{prior} , that represents an effective detection threshold combining previous SETI surveys. Depending on the detectors employed and their location, previous sky surveys covered different extended regions of the sky with flux thresholds ranging from about 10^{-22} W/m² to about 10^{-24} W/m² in the frequency range 1-2 GHz [24, 35–40]. Here we adopt a conservative value of $S_{\min}^{\text{prior}} = 10^{-23}$ Wm⁻², which brings about a maximum detectable radius of $R_{L^*}^{\text{prior}} = 0.0422 \sqrt{L^*/L_{\text{Arecibo}}}$ kly. In other terms, by adopting $S_{\min}^{\text{prior}} = 10^{-23}$ Wm⁻² we are ruling out the existence of detectable signals from emitters within ~ 40 ly from Earth that transmit within a frequency range 1-2 GHz with an EIRP equivalent to that of the Arecibo radar.

Even for $L^* = 100L_{\text{Arecibo}}$, the chosen $R_{L^*}^{\text{prior}}$ is well within the distance at which the probability of detecting an emitter luminosity is small and follows a power law. For a Dirac-delta luminosity function we estimate $\pi_o^{\text{prior}} = \pi_o(R_{L^*}^{\text{prior}}) \sim 2.6 \times 10^{-8} (L^*/L_{\text{Arecibo}})^{3/2}$ (SI Appendix, Section III). The corresponding value of k_{\min} follows from $\bar{k}_{\min} \simeq 0.14 \pi_o^{\text{prior}}$, as discussed above.

E. Posteriors

Figure 6 shows the posterior CCDFs of \bar{k} (solid lines) resulting from events \mathcal{E}_0 , $\bar{\mathcal{E}}_0$, and \mathcal{E}_1 computed using a Dirac-delta $g(L)$ and an EIRP of the emitters equal to that of the Arecibo radar ($L^* = L_{\text{Arecibo}}$). The area colored in gray encompasses the values that the posterior probability can take between the limiting events $\bar{\mathcal{E}}_0$ and \mathcal{E}_1 . Since the prior observational radius used to calculate the prior probability (dashed lines) refers to frequencies between 1 GHz and 2 GHz, the posteriors must be understood as referring to the same frequency range.

The results shown in Fig. 6A are computed for an observational radius containing about one million stars ($R_{L^*} = 500$ ly), which is the number of nearby targeted stars that the ‘‘Breakthrough Listen’’ program will search for radio emissions. Since the fractional volume of the Galaxy encompassed by this value of R_{L^*} is very small [$\pi_o(R_{L^*} = 500 \text{ ly}) \sim 10^{-5}$, Fig. 5A], the posterior CCDF resulting from the non-detection of signals (event \mathcal{E}_0) is not significantly smaller than the prior. While the inferred upper limit of \bar{k} ($\sim 1/\pi_o \sim 10^5$) is about two orders of magnitude smaller than that derived from our prior, the posterior probability that $\bar{k} \geq 1$ ($\sim 33\%$) is reduced by a factor of only 1.4. On the contrary, the posterior CCDFs resulting from the discovery of a signal within 500 ly differ considerably from the prior. We find a probability exceeding 97% that more than 10^3 signals typically cross our planet. Depending on whether we assign the signal detection to event \mathcal{E}_1 or event $\bar{\mathcal{E}}_0$, \bar{k} is bounded from above by $\sim 3 \times 10^5$ or $\sim 10^8$, respectively.

Extending the observational radius up to the galactic center ($R_{L^*} = 27$ kly, Fig. 6B) changes drastically the responses to events \mathcal{E}_0 , $\bar{\mathcal{E}}_0$, and \mathcal{E}_1 . Not detecting sig-

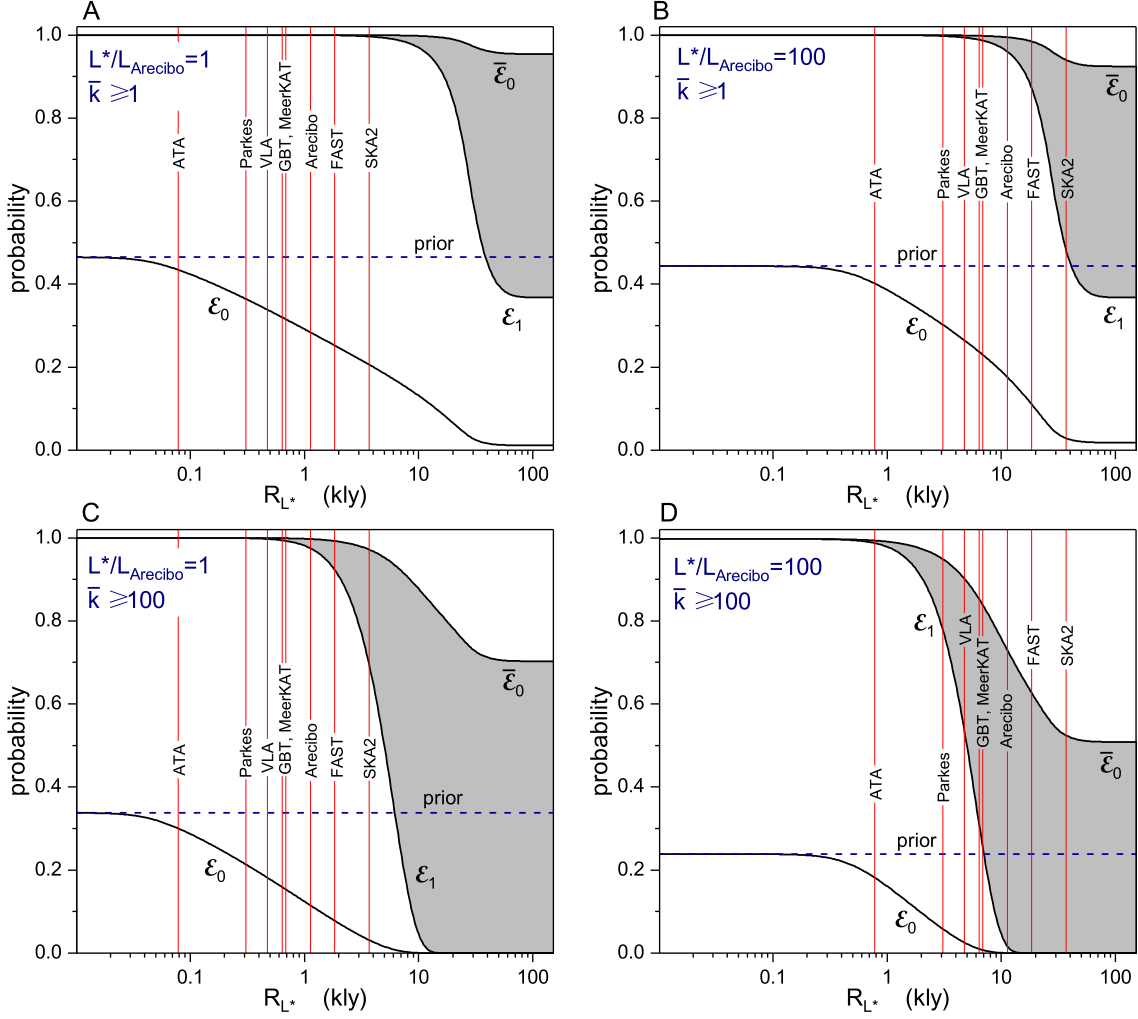


FIG. 7. Posterior probability that $\bar{k} \geq 1$ (top row) and $\bar{k} \geq 100$ (bottom row) for emitters with characteristic luminosity $L^*/L_{\text{Arecibo}} = 1$ (left column) and $L^*/L_{\text{Arecibo}} = 100$ (right column), where $L_{\text{Arecibo}} = 2 \times 10^{13}$ W is the EIRP of the Arecibo radar. Dashed lines denote the prior probabilities, while the solid curves are posterior probabilities as a function of the observational radius R_{L^*} resulting from the events of non-detection (\mathcal{E}_0), at least one detectable signal ($\bar{\mathcal{E}}_0$), and exactly one detectable signal (\mathcal{E}_1). The results have been obtained by assuming a Dirac-delta luminosity function centered at L^* . The red vertical lines indicate the values of R_{L^*} that are accessible to the telescopes listed in Table I.

nals out to 27 kly implies that there are practically zero chances that $\bar{k} \gtrsim 3$, and no more than typically 10 detectable signals are expected to populate the Galaxy if instead exactly one signal is discovered within that radius (event \mathcal{E}_1).

The impact of the observational radius highlighted in Fig. 6 is best illustrated in Fig. 7, where the posterior probabilities that $\bar{k} \geq 1$ (upper row) and $\bar{k} \geq 100$ (lower row) are plotted as a function of R_{L^*} for emitter luminosities centered at L_{Arecibo} (left column) and $100L_{\text{Arecibo}}$ (right column). The red vertical lines are the corresponding R_{L^*} values accessible to some of the detector facilities listed in Table I.

It is useful to discuss separately the cases in which R_{L^*} is smaller or larger than about 1 kly. In the former case,

the lack of signal detection, event \mathcal{E}_0 , does not imply a dramatic revision of the prior probability (dashed lines). For example, the posterior probability that $\bar{k} \geq 1$ is not smaller than about half the prior probability (top row of Fig. 7). This factor is somewhat reduced, but not significantly, if we consider the posterior probability that $\bar{k} \geq 100$, as shown in the bottom row of Fig. 7. Under the assumption that our prior correctly reflects the current state of knowledge, not detecting signals out to a distance of ~ 1 kly is still consistent with a probability larger than 10 % that there are typically more than 100 signals crossing Earth from Arecibo-like emitters ($L^* = L_{\text{Arecibo}}$, Fig. 7C) located in the entire Galaxy.

The discovery of a signal emitted within ~ 1 kly implies a dramatic revision of our prior assumptions, as the

posterior probability resulting from either $\bar{\mathcal{E}}_0$ or \mathcal{E}_1 collapses to one even for $\bar{k} \geq 100$. This occurs practically regardless of the assumed prior (Supplementary information). More generally, we find a posterior probability exceeding 95 % that more than $\sim 146(\text{kly}/R_{L^*})^3$ signals intersect the Earth in average. This estimate must be multiplied by a factor 2.5 if a uniform luminosity function is assumed (SI Appendix, Section IV).

In the case that R_{L^*} extends well beyond the galactic neighborhood, the lack of signal detection considerably shrinks the chances of discovering emitters from farther distances. In particular, the posterior probability that $\bar{k} \geq 1$ reduces to less than 2 % when $R_{L^*} \gtrsim 30 - 40$ kly (top row of Fig. 7). It follows that if the SKA2 telescope, or any other detector of comparable sensitivity, does not detect signals in an all-sky search, it is unlikely that any powerful emitter ($\sim 100L_{\text{Arecibo}}$) whose signal crosses Earth exists in the entire Galaxy, Fig. 7B. Yet, even if the SKA2 telescope reports null results, less powerful signals ($\sim L_{\text{Arecibo}}$) may still intersect the Earth with a significant probability (~ 20 %) that $\bar{k} \geq 1$, Fig. 7A, although the probability that $\bar{k} \geq 100$ drops to only about 3 %, Fig. 7C.

The response to the hypothetical discovery of a signal within observational radii larger or much larger than ~ 1 kly differ whether exactly one signal (event \mathcal{E}_1) or at least one signals (event $\bar{\mathcal{E}}_0$) is detectable within R_{L^*} . While in the former case the chances that $\bar{k} \geq 100$ drop exponentially to zero for $R_{L^*} \gtrsim 10$ kly, they remain significant in response to $\bar{\mathcal{E}}_0$ even when the observable sphere encompasses the entire Galaxy, as shown in Figs. 7C and 7D. If we take again the SKA2 telescope as an illustrative example, and assume that this telescope discovers a signal, it follows from Fig. 7D that the probability that there are still more than 100 powerful ($\sim 100L_{\text{Arecibo}}$) detectable emitters to be discovered ranges between ~ 52 % and 0 % as the examined portion of the sky grows from a small patch to the entire celestial sphere.

The use of a uniform luminosity function rather than a Dirac-delta does not change qualitatively the posterior probabilities of Figs. 6 and 7. Specifically, the responses to \mathcal{E}_0 and \mathcal{E}_1 are only slightly affected in the region well beyond the galactic neighborhood (Fig. S3). Our results are relatively robust also with respect to different choices of the prior observational radius. An effective detection threshold 10 times smaller than $S_{\text{min}}^{\text{prior}} = 10^{-23} \text{ Wm}^{-2}$ affects only the posterior resulting from the detection of a signal within ≈ 1 kly, which drops to 90 % if $L^* = 100L_{\text{Arecibo}}$ is assumed (Fig. S2 and S4).

A previous Bayesian analysis applied to a large set of targeted stars was done in Ref.[25]. We have improved on this approach by including detector sensitivity, the luminosity function of the emitters, and the density number function of stars in the Galaxy. Furthermore, the use of an uninformative prior, such as the log-uniform PDF used here, likely gives a more accurate posterior probabilities of detection (see footnote on page 4).

Finally, It is worth stressing that the inferred mean

number of signals crossing Earth shown in Fig. 7 represents a lower bound to the total number, qN_s , of signals populating the Galaxy, as illustrated in Fig. 2. For signal lifetimes smaller than $t_M \simeq 87,000$ years, the typical amount of galactic signals that do not cross our planet is larger than \bar{k} .

V. CONCLUSIONS

The present state of knowledge is insufficient to allow an informed estimate of the probability that non-natural EM signals emitted from the Milky Way intersects Earth's orbit. Yet, a theoretical approach is still possible by assuming potential outcomes of future, extensive SETI surveys. Evidence that no signals are detected within a certain distance from Earth, and within a certain window of frequencies, can be used as an input datum to infer, within a Bayesian statistical framework, the probability that emitters transmitting at comparable frequencies exist at further distances. The datum of non-detection has however a moderate informative value unless the sampled region contains a significant fraction of the Galaxy. The possibility that galactic, non-natural EM emissions as powerful as the Arecibo radar cross our planet can be reasonably ruled out only if no signals are observed within a radius of at least ~ 40 kly for Earth.

In the hypothesis that a SETI survey detects a genuinely non-natural extraterrestrial emission from nearby star systems, the inferred average number of signals crossing Earth is likely to be large. Under reasonable non-informed priors, a signal detected within a radius of ≈ 1 kly from Earth, emitted with an EIRP comparable to that of the Arecibo radar, implies almost a 100 % probability that, in average, more than ~ 100 signals of similar radiated power intersect the Earth. The total number of signals populating the Galaxy may be even larger because only a fraction of them is expected to cross our planet depending on the mean signal longevity, as shown in Fig. 2.

It is possible to improve the present formulation by relaxing a few assumptions that we have made. One of these is the presumed isotropy of the emission processes. It is not difficult however to formulate a model that includes a fraction of beam-like emissions, although their contribution to the total number of signals crossing Earth is marginal unless they are directed deliberately towards us [13].

Notwithstanding the importance that current and planned SETI efforts put in the search for radio signals, the optical and near-infrared spectrum [9] have recently gained a renewed interest [10–12]. Modeling the detection probability of signals at micrometer-submicrometer wavelengths requires that absorption and scattering processes of the interstellar medium are taken into account. In this case, the model should consider the spatial distribution of the galactic dust and the opacity coefficient, together with the aforementioned anisotropy of the emis-

sions.

In conclusion, we think that it is time to anticipate what forthcoming SETI surveys can potentially deliver in terms of informative data about the galactic population of non-natural emitters. A Bayesian approach appears to be the most appropriate tool to infer from data the typical amount of signals crossing Earth. As a last remark, we emphasize that the mean number of shell signals at Earth gives also the mean number of galactic civilizations currently emitting [14], enabling a possible empirical es-

timate of Drake's number directly from SETI data.

ACKNOWLEDGMENTS

We thank Amedeo Balbi, Thomas Basbøll, Frank Drake, Emilio Enriquez, Eric J. Korpela, Andrew Siemion, Jill Tarter, Nathaniel Tellis, and Dan Werthimer for fruitful discussions.

-
- [1] Enriquez JE, et al. (2017) The Breakthrough Listen search for intelligent life: 1.1-1.9 GHz observations of 692 nearby stars. *Astrophys J* 849:104.
 - [2] Petigura EA, Howard AW, Marcy GW (2013) Prevalence of earth-size planets orbiting sun-like stars. *Proc Natl Acad Sci USA* 110:19273-19278.
 - [3] Batalha NM, et al. (2013) Planetary candidates observed by Kepler. III. analysis of the first 16 months of data. *Astrophys J* 204:24.
 - [4] Isaacson H, et al. (2017) The Breakthrough Listen search for intelligent life: target selection of nearby stars and galaxies. *Publ Astron Soc Pac* 129:054501.
 - [5] Lazio TJW, Tarter JC, Wilner DJ (2004) The cradle of life. *New Astron Rev* 48:985-991.
 - [6] Siemion APV, et al. (2015) Searching for extraterrestrial intelligence with the Square Kilometre Array. *Advancing Astrophysics with the Square Kilometre Array (AASKA14)*, eds Bourke TL, et al. (International School for Advanced Studies, Trieste, Italy), Vol 215, no. 116.
 - [7] Loeb A, Zaldarriaga M (2007) Eavesdropping on radio broadcasts from galactic civilizations with upcoming observatories for redshifted 21 cm radiation. *J Cosmol Astropart Phys* 2007:20.
 - [8] Garrett MA, Siemion A, CappellenWA (2017) All-sky radio SETI. *MeerKAT Science: On the Pathway to the SKA (MeerKAT2016)*, eds Taylor P, Camilo F, Leeuw L, Moodley K (International School for Advanced Studies, Trieste, Italy), Vol 277, no. 020.
 - [9] Townes CH (1983) At what wavelengths should we search for signals from extraterrestrial intelligence? *Proc Natl Acad Sci USA* 80:1147-1151.
 - [10] Tellis NK, Marcy GW (2015) A search for optical laser emission using Keck HIRES. *Publ Astron Soc Pac* 127:540-551.
 - [11] Tellis NK, Marcy GW (2017) A search for laser emission with megawatt thresholds from 5600 FGKM stars. *Astron J* 153:251.
 - [12] Wright SA, et al. (2018) Panoramic optical and near-infrared SETI instrument: Overall specifications and science program. *Proceedings SPIE, Ground-based and Airborne Instrumentation for Astronomy VII, Proceedings of SPIE*, eds Evans CJ, Simard L, Takami H (SPIE, Bellingham, WA), Vol 10702, pp 107025H1-107025H12.
 - [13] Grimaldi C (2017) Signal coverage approach to the detection probability of hypothetical extraterrestrial emitters in the milky way. *Sci Rep* 7:46273.
 - [14] Grimaldi C, Marcy GW, Tellis NK, Drake F (2018) Area coverage of expanding E.T. signals in the galaxy: SETI and Drake's N. *Publ Astron Soc Pac* 130:054101.
 - [15] Balbi A (2018) The impact of the temporal distribution of communicating civilizations on their detectability. *Astrobiology* 18:5458.
 - [16] de Geus EJ, Vogel SN, Digel SW, Gruendl RA (1993) An H II region beyond the optical disk of the galaxy. *Astrophys J* 412:L97-L100.
 - [17] Anderson LD, et al. (2015) Finding distant galactic HII regions. *Astrophys J Suppl Ser* 221:26.
 - [18] Di Stefano R, Ray A (2016) Globular clusters as cradles of life and advanced civilizations. *Astrophys J* 827:54.
 - [19] Drake F (1961) Project Ozma. *Phys Today* 14:40-46.
 - [20] Drake F (1965) The radio search for intelligent extraterrestrial life. *Current Aspects of Exobiology*, eds Mamikunian G, Briggs MH (Pergamon Press, New York), pp 323-345.
 - [21] Trotta R (2008) Bayes in the sky: Bayesian inference and model selection in cosmology. *Contemp Phys* 49:71-104.
 - [22] Ward PD, Brownlee D (2000) *Rare Earth: Why Complex Life is Uncommon in the Universe*. (Copernicus Springer-Verlag, New York).
 - [23] Spiegel DS, Turner EL (2012) Bayesian analysis of the astrobiological implications of life's early emergence on Earth. *Proc Natl Acad Sci USA* 109:3957-400.
 - [24] Tarter J (2001) The search for extraterrestrial intelligence (SETI). *Annu Rev Astron Astrophys* 35:511-548.
 - [25] Harp GR, et al. (2016) SETI observations of exoplanets with the Allen Telescope Array. *Astronom J* 152:181.
 - [26] Gray RH, Mooley K (2017) A VLA search for radio signals from m31 and m33. *Astronom J* 153:110.
 - [27] Jonas JL, et al. (2018) The MeerKAT radio telescope. *MeerKAT Science: On the Pathway to the SKA (MeerKAT2016)*, eds Taylor P, Camilo F, Leeuw L, Moodley K (International School for Advanced Studies, Trieste, Italy), Vol 277, no. 001.
 - [28] Foster G, et al. (2018) Alfaburst: a commensal search for fast radio bursts with Arecibo. *Mon Notices Royal Astron Soc* 474:3847-3856.
 - [29] Nan R, et al. (2011) The five-hundred-meter aperture spherical radio telescope (FAST) project. *Int J Mod Phys D* 20:989-1024.
 - [30] Lazio TJW (2013) The Square Kilometre Array pulsar timing array. *Class Quantum Gravity* 30:224011.
 - [31] Misiriotis A, Xilouris EM, Papamastorakis J, Boumis P, Goudis CD (2006) The distribution of the ISM in the Milky Way - A three-dimensional large-scale model. *Astron Astrophys* 459:113-123.

- [32] Lineweaver CH, Fenner Y, Gibson BK (2004) The galactic habitable zone and the age distribution of complex life in the Milky Way. *Science* 303:597-62.
- [33] Gulkis S (1985) Optimum search strategies for randomly distributed CW transmitters. *The Search for Extraterrestrial Life: Recent Developments. International Astronomical Union Series*, ed Papagiannis MD (Springer, Dordrecht, The Netherlands), Vol 112, pp 411-417.
- [34] Shostak S (2000) SETI merit and the galactic plane. *Acta Astronaut* 46:649-654.
- [35] Wolfe JH, et al. (1981) SETI-The Search for Extraterrestrial Intelligence-Plans and Rationale in *Life in the Universe* (MIT Press, Cambridge, MA), pp 391-417.
- [36] Horowitz P, Sagan C (1993) Five years of project META: an all-sky narrow-band radio search for extraterrestrial signals. *Astrophys J* 415:218-235.
- [37] Colomb FR, Hurrell E, Olalde JC, Lemarchand GA (1993) SETI activities in Argentina. *Third Decennial US-USSR Conference on SETI. ASP Conference Series*, ed Shostak GS (Astronomical Society of the Pacific, San Francisco), Vol 47, pp 279-288.
- [38] Stootman FH, De Horta AY, Oliver CA, Wellington KJ (2000) The southern SERENDIP project. *A New Era in Bioastronomy. ASP Conference Series*, eds Lemarchand G, Meech K (Astronomical Society of the Pacific, San Francisco), Vol 213, pp 491-496.
- [39] Leigh D, Horowitz P (2000) Strategies, implementation and results of BETA. *A new Era in Bioastronomy. ASP Conference Series*, eds Lemarchand G, Meech K (Astronomical Society of the Pacific, San Francisco), Vol 213, pp 459-466.
- [40] Bowyer S, et al. (2016) The SERENDIP III 70 cm search for extraterrestrial intelligence. [arXiv:1607.00440](https://arxiv.org/abs/1607.00440).

Supplementary Information: Bayesian approach to SETI

Claudio Grimaldi^{1,*} and Geoffrey W. Marcy^{2,†}

¹Laboratory of Physics of Complex Matter, Ecole Polytechnique
Fédérale de Lausanne, Station 3, CP-1015 Lausanne, Switzerland

²University of California, Berkeley, CA 94720, USA

I. MEAN NUMBER OF SIGNALS

We denote N_s the number of stars in the Galaxy and assume that a fraction q of stars harbors communicating civilizations that have been actively transmitting some time within $t_M = R_M/c$ years from present. The conditional probability that a signal crosses Earth given that it has been transmitted within a time t_M from present is

$$p = q \frac{\int dL \rho_L(L) \int_0^{t_M+L} dt \rho_t(t) \int d\vec{r} \rho_s(\vec{r}) f_{R,\Delta}(\vec{r} - \vec{r}_o)}{N_s \int dL \rho_L(L) \int_0^{t_M+L} dt \rho_t(t)}, \quad (\text{S1})$$

where $f_{R,\Delta}(\vec{r} - \vec{r}_o) = \theta(R - |\vec{r} - \vec{r}_o|) \theta(|\vec{r} - \vec{r}_o| - R + \Delta)$ is the indicator function for the condition that the signal crosses Earth (located at \vec{r}_o), $R = ct$ and $\Delta = cL$ are respectively the outer radius and the thickness of the spherical shell signal, t and L are the starting time and the duration of the emission process, $\rho_t(t)$ and $\rho_L(L)$ are the probability distribution functions (PDFs) of respectively t and L , and $\rho_s(\vec{r})$ is the number density of stars.

We make the hypothesis that within a time t_M from present, the birthrate of the emissions is constant ($\rho_t(t) = \text{const.}$). In this way, after the integrations over t are performed, Eq. S1 reduces to:

$$p = q \frac{\int dL \rho_L(L) \int d\vec{r} \rho_s(\vec{r}) \theta(t_M + L - |\vec{r} - \vec{r}_o|/c) [\theta(t_M - |\vec{r} - \vec{r}_o|/c)L + \theta(|\vec{r} - \vec{r}_o|/c - t_M)(t_M + L - |\vec{r} - \vec{r}_o|/c)]}{N_s \int dL \rho_L(L)(L + t_M)}. \quad (\text{S2})$$

Since $\rho_s(\vec{r})$ is by construction exponentially small for $|\vec{r}| > R_G$, where $R_G \sim 60$ kly is the galactic radius, $|\vec{r} - \vec{r}_o|$ is limited by $R_M = ct_M = R_G + r_o$. We can therefore set $\theta(t_M - |\vec{r} - \vec{r}_o|/c) = 1$ in Eq. S2 to obtain:

$$p = q \frac{\int dL \rho_L(L) \int d\vec{r} \rho_s(\vec{r}) L}{N_s \int dL \rho_L(L)(L + t_M)} = q\lambda, \quad (\text{S3})$$

where we have used $\int d\vec{r} \rho_s(\vec{r}) = N_s$, $\lambda = \bar{L}/(\bar{L} + t_M)$ is the scaled longevity of the signal, and $\bar{L} = \int dL \rho_L(L)L$ is the average signal duration. Since $p = q\lambda$ is the probability that a signal from the Galaxy crosses Earth, and given that there are N_s star systems in the Milky Way, the mean number of signals intercepting Earth is:

$$\bar{k} = q\lambda N_s. \quad (\text{S4})$$

Now we show that, in the steady state, \bar{k} coincides with the mean number of galactic civilizations that are currently transmitting, regardless of whether or not their signals intersect the Earth. The condition that an emitter is currently transmitting requires that its emission process lasts for a time L longer than the starting time t . Under the steady

* claudio.grimaldi@epfl.ch

† geoff.w.marcy@gmail.com

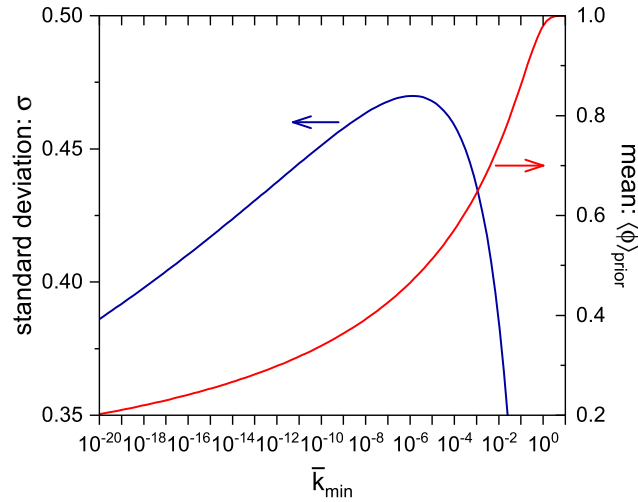


FIG. S1. Expected value $\langle \phi \rangle_{\text{prior}}$ that at least one signal crosses Earth (red curve, right scale) and the corresponding standard deviation σ (blue curve, left scale) obtained from the prior PDF of Eq. S6 as the cut-off \bar{k}_{min} varies.

state hypothesis $\rho_t(t) = \text{constant}$, the probability p_{curr} that an emitter is currently transmitting is therefore:

$$\begin{aligned}
 p_{\text{curr}} &= q \frac{\int dL \rho_L(L) \int_0^{t_M+L} dt \rho_t(t) \int d\vec{r} \rho_s(\vec{r}) \theta(L-t)}{N_s \int dL \rho_L(L) \int_0^{t_M+L} dt \rho_t(t)} \\
 &= q \frac{\int dL \rho_L(L) L}{\int dL \rho_L(L) (L + t_M)} = q\lambda,
 \end{aligned} \tag{S5}$$

from which we recover Eq. S3. The mean number of active emitters is thus $\bar{k}_{\text{curr}} = p_{\text{curr}} N_s = q\lambda N_s$, which coincides with Eq. S4.

II. PRIOR DETECTION PROBABILITY

Criterion for the choice of \bar{k}_{min}

The prior probability density distribution (PDF) used in this study is:

$$p(\bar{k}) = \frac{\bar{k}^{-1} e^{-\pi_o^{\text{prior}} \bar{k}}}{E_1(\pi_o^{\text{prior}} \bar{k}_{\text{min}})} \theta(\bar{k} - \bar{k}_{\text{min}}), \tag{S6}$$

where $E_1(x) = \int_x^\infty dt e^{-t}/t$ is the exponential integral, π_o^{prior} is the probability that previous SETI surveys detect the luminosity of an emitter, and \bar{k}_{min} is a lower cut-off for the mean value of galactic isotropic signals crossing Earth. While the value of π_o^{prior} (or at least its order of magnitude) can be roughly estimated by looking at the probe sensitivities and the portion of sky covered by previous SETI searches, \bar{k}_{min} can be chosen by requiring that Eq. S6 represents a fairly non-informative prior.

To guide our choice for a suitable value of \bar{k}_{min} , it is instructive to consider first the probability, denoted ϕ , that at least one signal from the entire Galaxy intercepts the Earth. From the Poisson degree distribution $p(k)$ we find that:

$$\phi = 1 - p(0) = 1 - e^{-\bar{k}}. \tag{S7}$$

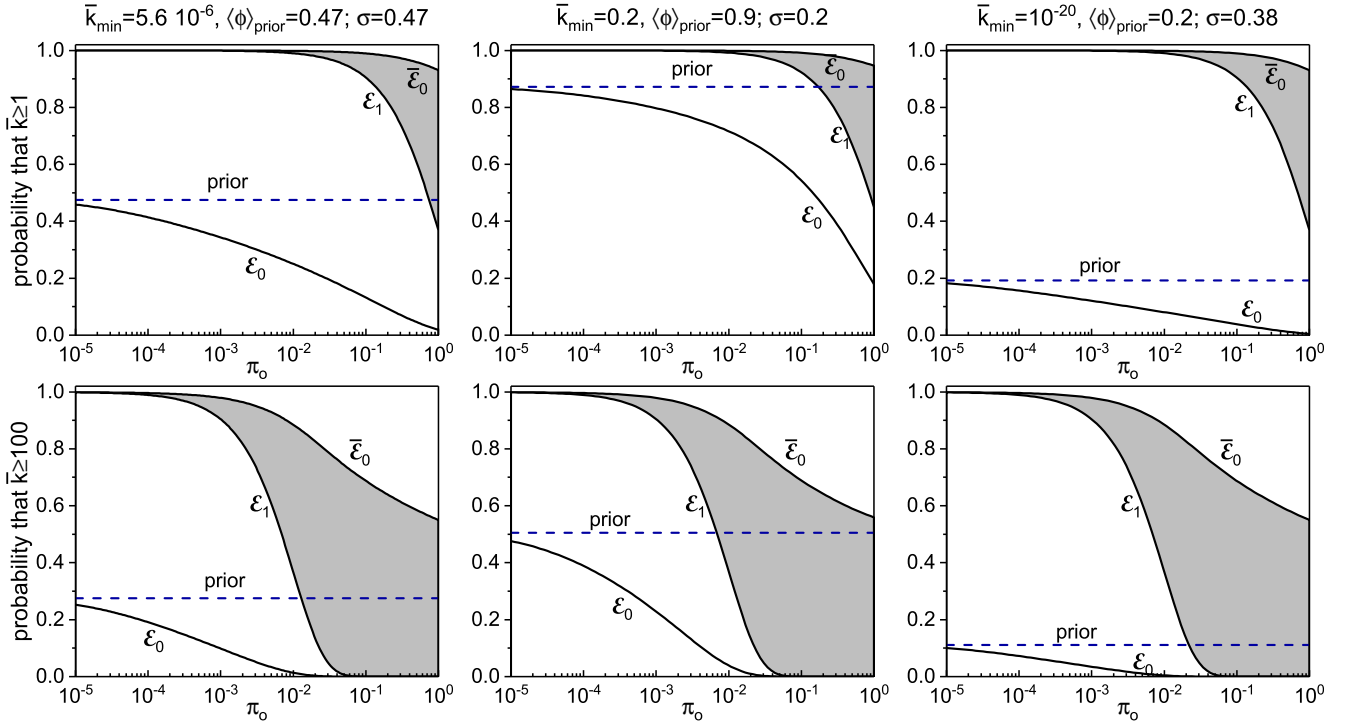


FIG. S2. Posterior probability that there 1 or more (top row) and 100 or more (bottom row) signals intercepting Earth as a function of the luminosity detection probability π_o and for different values of \bar{k}_{\min} . The horizontal dashed lines denote the corresponding prior probabilities, while the solid curves are the posteriors resulting from the events of non-detection (\mathcal{E}_0), at least one detectable signal ($\bar{\mathcal{E}}_0$), and exactly one detectable signal (\mathcal{E}_1). The grey region comprised between the posteriors of $\bar{\mathcal{E}}_0$ and \mathcal{E}_1 represents the possible values of the posterior probability resulting from the event of signal detection.

The expected value of ϕ under the assumption that \bar{k} is distributed according to the prior PDF of Eq. S6 is:

$$\langle \phi \rangle_{\text{prior}} = \int_0^{\infty} d\bar{k} (1 - e^{-\bar{k}}) p(\bar{k}) = 1 - \frac{E_1[(1 + \pi_o^{\text{prior}}) \bar{k}_{\min}]}{E_1(\pi_o^{\text{prior}} \bar{k}_{\min})}. \quad (\text{S8})$$

Since $E_1(x) \simeq \ln(1/x) - \gamma$ for $x \rightarrow 0$, where $\gamma = 0.5772\dots$ is Euler's constant, a vanishing cut-off $\bar{k}_{\min} \rightarrow 0$ implies that $\langle \phi \rangle_{\text{prior}} = 0$. In this limit $\bar{k}_{\min} \rightarrow 0$, therefore, the prior S6 turns out to be highly informative because it privileges scenarios in which there are no signals crossing Earth. As $\bar{k}_{\min} > 0$, however, $\langle \phi \rangle_{\text{prior}}$ becomes different from zero, as shown in Fig. S1 where Eq. S8 is calculated for $\pi_o^{\text{prior}} = 10^{-5}$. The figure shows also the standard deviation of ϕ obtained from the prior S6:

$$\begin{aligned} \sigma &= \sqrt{\langle \phi^2 \rangle_{\text{prior}} - \langle \phi \rangle_{\text{prior}}^2} \\ &= \sqrt{\frac{E_1[(2 + \pi_o^{\text{prior}}) \bar{k}_{\min}]}{E_1(\pi_o^{\text{prior}} \bar{k}_{\min})} - \frac{E_1[(1 + \pi_o^{\text{prior}}) \bar{k}_{\min}]^2}{E_1(\pi_o^{\text{prior}} \bar{k}_{\min})^2}}. \end{aligned} \quad (\text{S9})$$

If we take as a measure of the prior non-informativeness the spread of ϕ , the least informative prior PDF is thus identified by the value of \bar{k}_{\min} such that the standard deviation σ is maximum. In the example of Fig. S1, σ is maximum when $\bar{k}_{\min} \simeq 1.3 \times 10^{-6}$, to which it corresponds $\langle \phi \rangle_{\text{prior}} \simeq 0.47$. In general, the value of \bar{k}_{\min} for which σ is maximum can be calculated by asking that $d\sigma/d\bar{k}_{\min} = 0$, which for $\pi_o^{\text{prior}} \ll 1$ leads to

$$\ln(C \bar{k}_{\min}) \simeq \ln(\pi_o^{\text{prior}}) \frac{\ln(\pi_o^{\text{prior}}/2)}{\ln(2\pi_o^{\text{prior}})} \simeq \ln(\pi_o^{\text{prior}}/4), \quad (\text{S10})$$

where $C = \exp(\gamma) \simeq 1.78$. Hence $\bar{k}_{\min} \simeq \pi_o^{\text{prior}}/4C \simeq 0.14\pi_o^{\text{prior}}$.

Effects of \bar{k}_{\min} on the posterior probabilities

To see how the posteriors are affected by choices of \bar{k}_{\min} that give large or small values of $\langle\phi\rangle_{\text{prior}}$, we calculate the posterior probabilities that $\bar{k} \geq 1$ and $\bar{k} \geq 100$ obtained by setting $\bar{k}_{\min} = 0.56\pi_o^{\text{prior}} = 5.6 \times 10^{-6}$ (i.e., the noninformed prior used in the main text), $\bar{k}_{\min} = 0.2$ ($\langle\phi\rangle_{\text{prior}} \simeq 0.9$), and $\bar{k}_{\min} = 10^{-20}$ ($\langle\phi\rangle_{\text{prior}} \simeq 0.2$).

Figure S2 shows that the posteriors resulting from the detection of a signal (events $\bar{\mathcal{E}}_0$ and \mathcal{E}_1) are hardly affected by \bar{k}_{\min} and are thus not conditioned by the prior, even if \bar{k}_{\min} is chosen so as to privilege large or small values of \bar{k} (or, equivalently, large or small values of $\langle\phi\rangle_{\text{prior}}$).

In contrast, the probability value inferred by the lack of signal detection (event \mathcal{E}_0 , lower solid lines in Fig. S2) depend on the assumed prior, because in the limit $\pi_o \rightarrow 0$ the two must coincide. As a consequence, for each case of Fig. S2 a substantial effect of the event \mathcal{E}_0 has to be expected only for values of π_o significantly larger than π_o^{prior} . Note however that the posteriors due to the event of non-detection become negligible when $\bar{k} > 1/\pi_o$, regardless of the assumed priors. For example, the probability that there are more than ~ 100 signals crossing Earth vanishes exponentially when $\pi_o \gtrsim 0.01$, as shown in the lower panels of Fig. S2.

III. LIMITING BEHAVIOR OF π_o AT SMALL R_L^*

The probability that the luminosity of an emitter is detectable [introduced in Eq. (8) of the main text] can be rewritten as:

$$\pi_o(R_L^*) = \int_0^{L^*} dL g(L) \tilde{\pi}_o(R_L) \quad (\text{S11})$$

where $g(L)$ is the luminosity function, L^* is a maximum luminosity threshold, and

$$\tilde{\pi}_o(R_L) = \frac{1}{N_s} \int d\vec{r} \rho_s(\vec{r}) \theta(R_L - |\vec{r} - \vec{r}_o|) \quad (\text{S12})$$

is the probability that an emitter is within a distance $R_L = \sqrt{L/4\pi S_{\min}}$ from Earth, where S_{\min} is the sensitivity of the detector. In Eq. S12 $\rho_s(\vec{r})$ is the number density of stars in the Galaxy, \vec{r} is the position vector of the emitter relative to the galactic center, and \vec{r}_o is the position vector of the Earth. For R_L much smaller than the typical length scale over which $\rho_s(\vec{r})$ varies, we approximate Eq. S12 as follows:

$$\tilde{\pi}_o(R_L) \simeq \frac{\rho_s(\vec{r}_o)}{N_s} \int d\vec{r} \theta(R_L - |\vec{r} - \vec{r}_o|) = \frac{4\pi}{3} \frac{\rho_s(\vec{r}_o)}{N_s} R_L^3, \quad (\text{S13})$$

which shows that $\tilde{\pi}_o(R_L)$ is proportional to R_L^3 .

To get an explicit formula for Eq. S13, we consider the following expression:

$$\frac{\rho_s(\vec{r})}{N_s} = \frac{(r/r_s)^\beta e^{-r/r_s} e^{-|z|/z_s}}{4\pi r_s^2 z_s \Gamma(\beta + 2)}, \quad (\text{S14})$$

where $\beta \geq 0$, r is the radial distance from the galactic center, z is the height from the galactic plane, and Γ is the Gamma function. The above expression is more general than that considered in the main text because depending on the value of β and r_s the radial dependence can be changed so as to reproduce different galactic distributions of those stars thought to have more chances to develop life. In general, the form of $\rho_s(\vec{r})$ can be chosen to represent the galactic habitable zone (GHZ) which takes into account factors such as the star metallicity and the rate of major sterilizing events (e.g., supernovae) that are thought to be important for the development of life. We consider two models for the GHZ: in the first one we set $\beta = 0$, $r_s = 8.15$ kly, and $z_s = 0.52$ kly, which gives a GHZ extending over the entire thin disk of the Galaxy. In the second model, we take an annular shape for the GHZ by choosing $\beta = 7$, $r_s = 3.26$ kly, and $z_s = 0.52$ kly.

Since the Sun lies approximately on the galactic plane ($z \simeq 0$ kly) and its radial distance from the center of the Milky Way is about $r_o = 27$ kly, we obtain from Eqs. S13 and S14:

$$\tilde{\pi}_o(R_L) \simeq \frac{(r_o/r_s)^\beta e^{-r_o/r_s}}{3r_s^2 z_s \Gamma(\beta + 2)} R_L^3 = \left(\frac{R_L}{a}\right)^3, \quad (\text{S15})$$

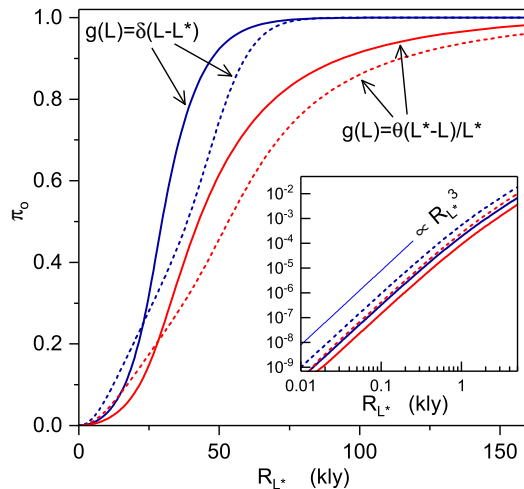


FIG. S3. Probability π_o that an emitter is within an observable sphere of radius R_{L^*} for the cases in which the emitter luminosity function is either a single Dirac-delta peak centered at L^* or a uniform distribution extending up to L^* . The solid and dashed line refer to a GHZ having disk-like and annular-like shape. The inset shows that within the galactic neighborhood ($R_{L^*} \lesssim 1$ kly) π_o scales as $R_{L^*}^3$

where

$$a = \begin{cases} 14.17 \text{ kly,} & \text{disk-like GHZ} \\ 9.96 \text{ kly,} & \text{annular-like GHZ} \end{cases} \quad (\text{S16})$$

The two model luminosity functions considered in the main text are either a Dirac-delta peak centered at L^* , $g(L) = \delta(L - L^*)$, or a uniform distribution of the form $g(L) = \theta(L^* - L)/L^*$, where $\theta(x)$ is the Heaviside step function. By introducing $R_{L^*} = \sqrt{L^*/4\pi S_{\min}}$, the maximum distance beyond which an emitter is instrumentally undetectable, in the limit $R_{L^*} \ll a$ Eq. S11 reduces for these two cases to:

$$\pi_o(R_{L^*}) = \eta \left(\frac{R_{L^*}}{a} \right)^3, \quad \eta = \begin{cases} 1, & \text{Dirac-delta } g(L) \\ 2/5, & \text{uniform } g(L) \end{cases} \quad (\text{S17})$$

Figure S3 shows the probability $\pi_o(R_{L^*})$ resulting from the disk-like and annular-like models of the GHZ for both a Dirac-delta and a uniform luminosity function $g(L)$. As shown in the inset, $\pi_o(R_{L^*})$ is proportional to $R_{L^*}^3$ regardless of the form of the GHZ. The figure shows also that the broadness of $g(L)$ has a more important effect than the shape of the GHZ.

IV. POSTERIOR PROBABILITY OF \bar{k} RESULTING FROM SIGNAL DETECTION WITHIN $R_{L^*} \lesssim 1$ KLY

Let us consider the posterior probability $\mathcal{P}(\bar{k}, \mathcal{E}_1)$ that the mean number of signals crossing Earth is larger than \bar{k} , given the evidence \mathcal{E}_1 that there is exactly one detectable signal. By taking $\mathcal{P}(\bar{k}, \mathcal{E}_1)$ equal to x , from Eq. (19) of the main text we obtain:

$$e^{-[\pi_o(R_{L^*}) + \pi_o(R_{L^*}^{\text{prior}})](\bar{k} + \bar{k}_{\min})} = x. \quad (\text{S18})$$

For $\bar{k} \gg \bar{k}_{\text{prior}}$, $\pi_o(R_{L^*}) \gg \pi_o(R_{L^*}^{\text{prior}})$, and $R_{L^*} \lesssim 1$ kly the above expression gives:

$$\eta \left(\frac{R_{L^*}}{a} \right)^3 \bar{k} = \ln \left(\frac{1}{x} \right), \quad (\text{S19})$$

where we have used Eqs. S17. Since $\mathcal{P}(\bar{k}, \mathcal{E}_1)$ is always smaller than $\mathcal{P}(\bar{k}, \mathcal{E}_0)$, we obtain that the detection of a signal implies a posterior probability larger than x that the mean number of signals at Earth exceeds

$$\bar{k} = \frac{1}{\eta} \left(\frac{a}{R_{L^*}} \right)^3 \ln \left(\frac{1}{x} \right). \quad (\text{S20})$$

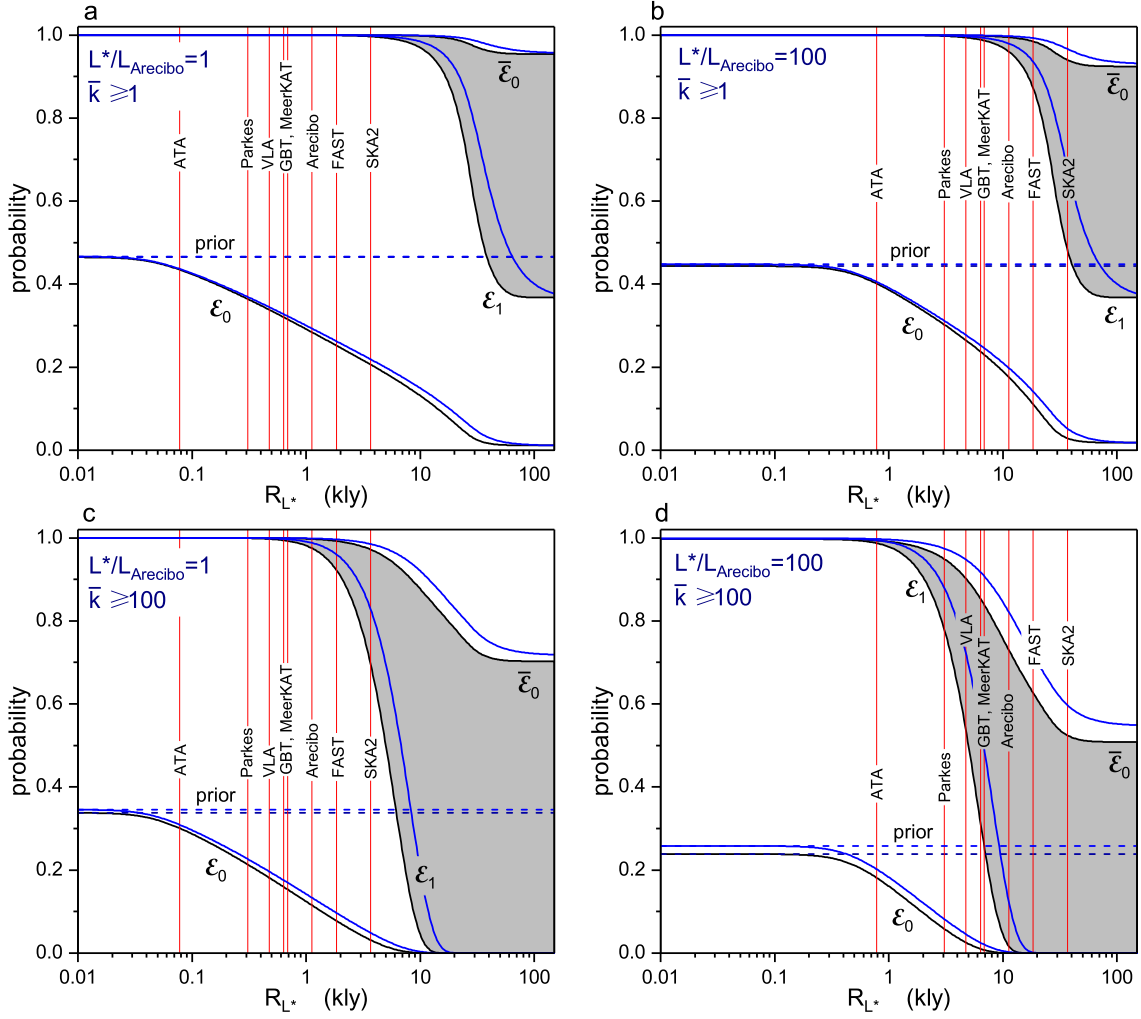


FIG. S4. Posterior probability that $\bar{k} \geq 1$ (top row) and $\bar{k} \geq 100$ (bottom row) for emitters with characteristic luminosity $L^*/L_{\text{Arecibo}} = 1$ (left column) and $L^*/L_{\text{Arecibo}} = 100$ (right column), where $L_{\text{Arecibo}} = 2 \times 10^{13}$ W is the EIRP of the Arecibo radar. Dashed lines denote the prior probabilities, while the solid curves are posterior probabilities as a function of the observable radius R_{L^*} resulting from the events of non-detection (\mathcal{E}_0), at least one detectable signal ($\bar{\mathcal{E}}_0$), and exactly one detectable signal (\mathcal{E}_1). Black curves are the results for a Dirac-delta luminosity function centered at L^* (as in Fig. 5 of the main text), while the blue curves have been calculated using a luminosity function that is constant between $L = 0$ and $L = L^*$ and zero otherwise. All cases have been obtained for a disk-like GHZ. The red vertical lines indicate the values of R_{L^*} that are accessible to the probes listed in Table 1 of the main text.

For $x = 0.95$ and using Eq. S16 the right-hand side of the above expression reduces to $\sim 146(\text{kly}/R_{L^*})^3$ and $\sim 50(\text{kly}/R_{L^*})^3$ for a disk-like and an annular-like GHZ, respectively.

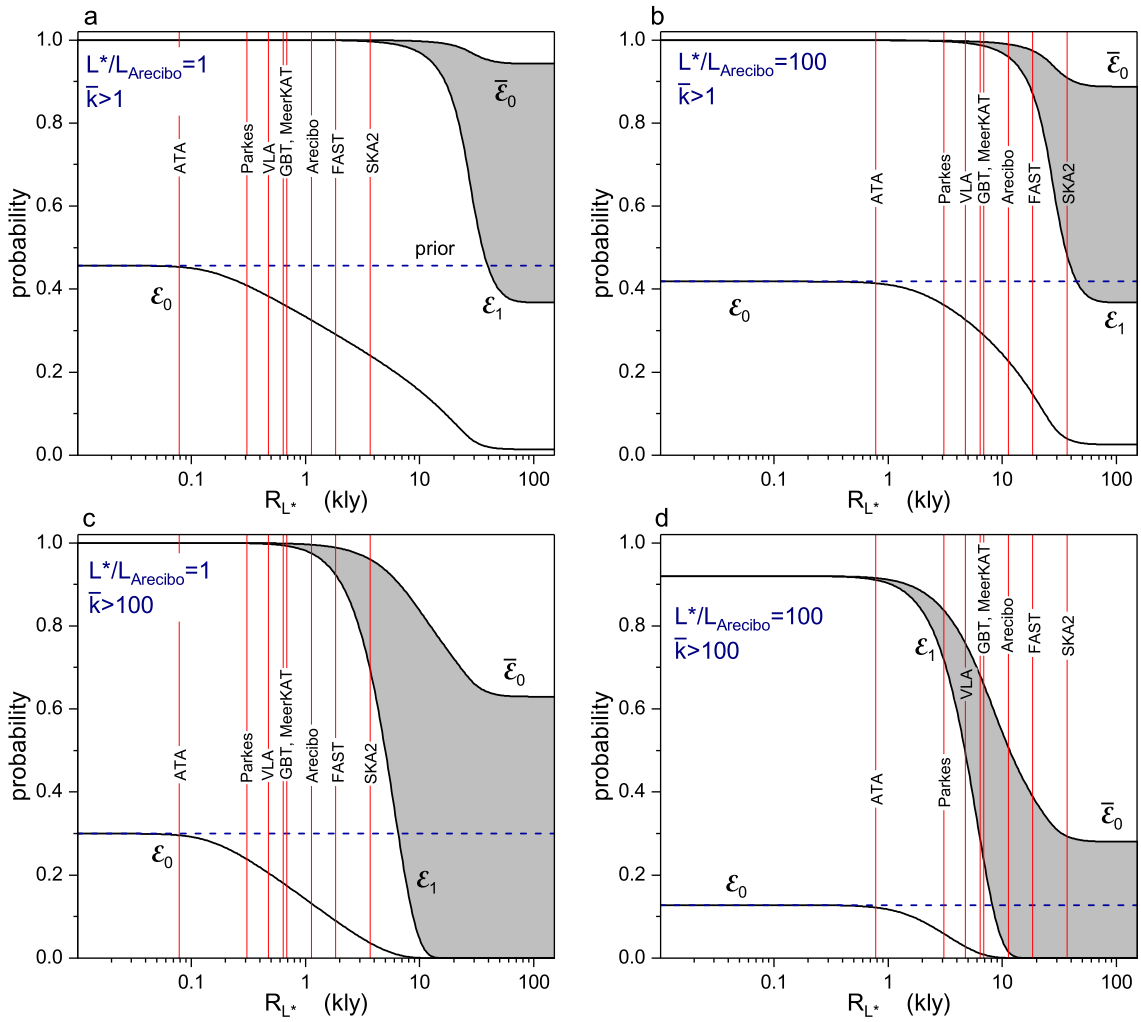


FIG. S5. Posterior probability that $\bar{k} \geq 1$ (top row) and $\bar{k} \geq 100$ (bottom row) for emitters with characteristic luminosity $L^*/L_{\text{Arecibo}} = 1$ (left column) and $L^*/L_{\text{Arecibo}} = 100$ (right column), where $L_{\text{Arecibo}} = 2 \times 10^{13}$ W is the EIRP of the Arecibo radar. The results have been obtained by using $S_{\text{min}}^{\text{prior}} = 10^{-24}$ Wm $^{-1}$, that is, 10 times smaller than that used in Fig. 5 of the main text. Dashed lines denote the prior probabilities, while the solid curves are posterior probabilities as a function of the observable radius R_{L^*} resulting from the events of non-detection (\mathcal{E}_0), at least one detectable signal ($\bar{\mathcal{E}}_0$), and exactly one detectable signal (\mathcal{E}_1). The results have been obtained by assuming a disk-like GHz and a Dirac-delta luminosity function centered at L^* . The red vertical lines indicate the values of R_{L^*} that are accessible to the probes listed in Table 1 of the main text.